where V is the velocity in the coordinate system rotating with the uniform velocity of the primaries about the center of mass, and

$$2\Omega = \xi^2 + \eta^2 + \zeta^2 + \frac{2(1-\mu)}{r_1} + \frac{2\mu}{r_2}$$

where ξ, η, and ζ are the coordinates of the particle in the same system, and r_1 and r_2 are the distances from the primaries of mass $1-\mu$ and μ, respectively (*4*).

When the primaries are in an elliptical orbit, the rate of rotation of the coordinate system becomes nonuniform, and the distance between the primaries in the dimensionless system also varies. Under these conditions, the Jacobian integral of the circular restricted problem must be replaced by the trajectory-dependent expression

$$C = \frac{2\Omega}{1 + E\cos f} - V^2 - 2(1-E^2)^{3/2}\int_{f_1}^{f_2} \frac{\Omega}{(1+E\cos f)^2} \cdot [E\sin f - E^2 \sin 2f + \cdots]\, df \qquad (1)$$

This expression can be transformed to a coordinate system centered upon the planet by a procedure similar to that used in deriving the Tisserand criterion for the identity of comets (*5*).

For qualitative evaluation of the possibilities of capture, the integral term in Eq. 1 may be omitted. However, for precise calculations of the dimensions of a captured satellite orbit, this approach is insufficient, since it neglects the fact that the primaries will cover some finite portion of their orbit, expressed by the limits f_1 and f_2 of the integral, during the process of capture.

It is therefore necessary to evaluate the integral along the path of capture. The required expansions for this have been derived and give the following relationships from which the dimensions of the capture orbits for Jupiter may be obtained. For satellites captured into direct orbits at perihelion

$$\frac{\mu}{a} = \frac{2}{1-E^2}\left(\frac{1}{1-\alpha} + \frac{\mu}{\alpha} - 1\right) + \frac{(1-\alpha)^2(1+E)^2}{1+E} - (1-E^2)^2 + 2\Omega\,[E - 2E^2 + E^3 - 2E^4 + \cdots] \qquad (2)$$

and for capture into retrograde orbits at aphelion

$$\frac{\mu}{a} - 4\sqrt{\mu a(1-e^2)}\cos i + 4a^2 = \frac{2}{1-E^2}\left(\frac{1}{1-\alpha} + \frac{\mu}{\alpha} - 1\right) + \frac{(1-\alpha)^2(1+E)^2}{1-E} - (1-E^2)^2 - 2\Omega\,[E + 2E^2 + E^3 + 2E^4 + \cdots] \qquad (3)$$

where μ and E are the mass ratio and eccentricity of the planet and α is the fractional distance of the Lagrangian point from the planet; Ω is derived from the value of the function Ω along the path of capture; and a, e, and i are the semimajor axis, eccentricity, and inclination, respectively, of the capture orbit.

We have $E = 0.048332$ as the present value of the orbital eccentricity of Jupiter, $\mu = 0.000954763$, and $\alpha = 0.0666931$. Also $2\Omega = 3.0978485$ and 3.0532237 for perihelion and aphelion captures, respectively. This gives a value of 0.01475 in dimensionless units for the semimajor axis of the direct capture orbits when Jupiter is at perihelion. When a value of 5.203 astronomical units (A.U.) for the semimajor axis of Jupiter is assumed, this corresponds to semimajor axes of 11.48×10^6 km for the direct capture orbits. Similarly, a value of 21.71×10^6 km is obtained for the retrograde orbits when Jupiter is at aphelion.

The 12 satellites of Jupiter are listed in Table 1, with values for the approximate diameters of the satellites and the semimajor axes, eccentricities, and inclinations of the orbits. It can be seen that the outer group, Jupiter VI, VII, and X, in direct orbits of considerable eccentricity and inclination and with semimajor axes of 11.47, 11.74, and 11.85×10^6 km, respectively, correspond closely to the predicted value of 11.48×10^6 km for capture into direct orbits while Jupiter is at perihelion.

The second group of outer satellites, Jupiter VIII, IX, XI, and XII, are in retrograde orbits of high eccentricity and inclination at distances of 23.5, 23.7, 22.5, and 21.2×10^6 km from the planet; this group probably represents satellites captured at aphelion, for which retrograde orbits having semimajor axes of 21.7×10^6 km are predicted.

The heliocentric coordinates necessary for an object to be captured by Jupiter may be derived by utilizing the criterion that the object must enter the inner Lagrangian point at perihelion or aphelion with zero velocity. It is found that the direct capture orbits at Jupiter perihelion correspond to bodies that had semimajor axes of 2.7836 A.U. and eccentricity of 0.5989. Similarly, the retrograde capture orbits are related to objects that had eccentricities close to 0.4972 and semimajor axes of 3.1517 A.U. Since this range of orbital parameters encompasses that corresponding to the asteroid belt, it seems that the seven outer satellites are probably captured asteroids.

J. MARTYN BAILEY
Graduate School of Arts and Sciences, George Washington University, Washington, D.C. 20005

References and Notes

1. J. M. Bailey, *Trans. Amer. Geophys. Union* **52**, 269 (1971); *J. Geophys. Res.*, in press.
2. This is related to the fact that capture may occur only if the satellite enters the inner Lagrangian point with zero relative velocity in a coordinate system rotating with the primaries. Two bodies in elliptical orbits, where one is restricted to remaining within the curve of zero velocity around the other, may have zero relative velocity only at perihelion or aphelion since only at these times can the orbits become tangent.
3. Physical characteristics and orbital parameters of Jupiter's satellites are from C. W. Allen, *Astrophysical Quantities* (Athlone, London, ed. 2, 1963), p. 68.
4. S. W. McCuskey, *Introduction to Celestial Mechanics* (Addision-Wesley, Reading, Mass., 1963).
5. F. F. Tisserand, *Traité de Méchanique Céleste* (Gauthier-Villars, Paris, 1896), vol. 4, p. 203.
6. Supported by NSF grant G.U. 3287.

10 May 1971

Antarctic Bottom Water: Major Change in Velocity during the Late Cenozoic between Australia and Antarctica

Abstract. *Paleomagnetic and micropaleontological studies of deep-sea sedimentary cores between Australia and Antarctica define an extensive area centered in the south Tasman Basin, where sediment as old as Early Pliocene has been systematically eroded by bottom currents. This major sedimentary disconformity has been produced by a substantial increase in velocity of Antarctic bottom water, possibly associated with late Cenozoic climatic cooling and corresponding increased glaciation of Antarctica.*

Studies of past oceanic circulation patterns have been restricted almost entirely to those changes in surface-water distributions indicated by fossil planktonic organisms (*1*). Changes in distribution and activity of deep-water masses have received little attention except where they are related to broad-scale, seismically defined changes in sediment patterns (*2*). Antarctic bottom water, which is produced under glaciated Antarctic conditions, plays an important role in oceanic circulation, since its formation creates transportation of new, oxygen-rich waters to the deep ocean basins in the world, thus inhibiting stagnation (*3*).

As water velocity is related to grain size, structures, and erosional and depositional history of sediments (*4*), estimates can be made of variations among these parameters. Until recently, only surface sediments were amenable to regional comparisons of current velocities because of the unique, apparently isochronous plane of observation provided (*4*). Paleomagnetic dating with micropaleontological control now enables such studies to be extended to subsurface isochronous planes, or to fine definition of possible diachronous relations of such planes. In this report we examine a series of deep-sea sedimentary cores from the Southern Ocean between Australia and Antarctica (Fig. 1) for evidence of past changes in the velocity of Antarctic bottom water. This represents an ideal area for such an examination because of the strong regional topographic control of bottom waters.

The cores used were collected during cruises 27 to 39 of U.S.N.S. *Eltanin* (Table 1 and Figs. 1 and 2). These form less than 20 percent of the total number of cores from the southwest Pacific, which are included in a more comprehensive analysis to be published elsewhere (*5*). The relevant shipboard operations and the paleomagnetic and micropaleontological methods have been described previously (*6*).

Sediment type in the cores varies greatly. It includes lutite, siliceous and carbonate ooze, and glacial marine material. Each core was sampled at 10-cm intervals. All specimens were demagnetized in alternating magnetic fields prior to measurement of remanent magnetism. The resulting paleomagnetic data for each core are shown in Fig. 2 as a function of age, which has been micropaleontologically verified. Actual core lengths, from which sedimentation rates can be calculated, are given in Table 1. Clearly, the known polarity history for the past few million years (*7*) is not ideally recorded in any cores, a fact that emphasizes the critical role of micropaleontological control of the ages defined. Material as old as Gilbert epoch is identified. Both planktonic Foraminifera and Radiolaria were examined to provide the micropaleontological control. The correlation lines for the major polarity boundaries have been placed by applying the radiolarian zonation established by Opdyke *et al.* (*8*) and Hays and Opdyke (*9*), and the foraminiferal zonation of Kennett (*10*).

The radiolarian species that were particularly valuable in our correlations were *Triceraspyris* sp. and *Lychnocanium grande* in the early and middle Gilbert; *Desmospyris spongiosa* (the extinction of which coincides approximately with the Gauss-Matuyama boundary); *Eucyrtidium calvertense* and *Clathrocyclas bicornis* (the extinction of which occurs in the middle Matuyama); and *Saturnulus planetes*, which in sub-Antarctic waters disappeared near the Brunhes-Matuyama boundary ($t = 0.69$ million years). The foraminiferal species that were particularly valuable in our correlations were *Globorotalia inflata* and *G. crassaformis*, whose appearance in sub-Antarctic waters is closely associated with the Brunhes-Matuyama boundary. Paleontological control for the shorter duration magnetic polarity events (Fig. 2) is often not available, especially for the events within the Gilbert epoch, where detailed paleontological control has yet to be established. Correlations of events are therefore made subjectively with use of the magnetic data alone, by comparison with the established geomagnetic polarity scale (*7*). In many of the cores, micropaleontological samples from near the top, middle, and bottom were sufficient to confirm paleomagnetic dating. In others, samples were examined at closer intervals for adequate dating, or for defining the position of disconformities.

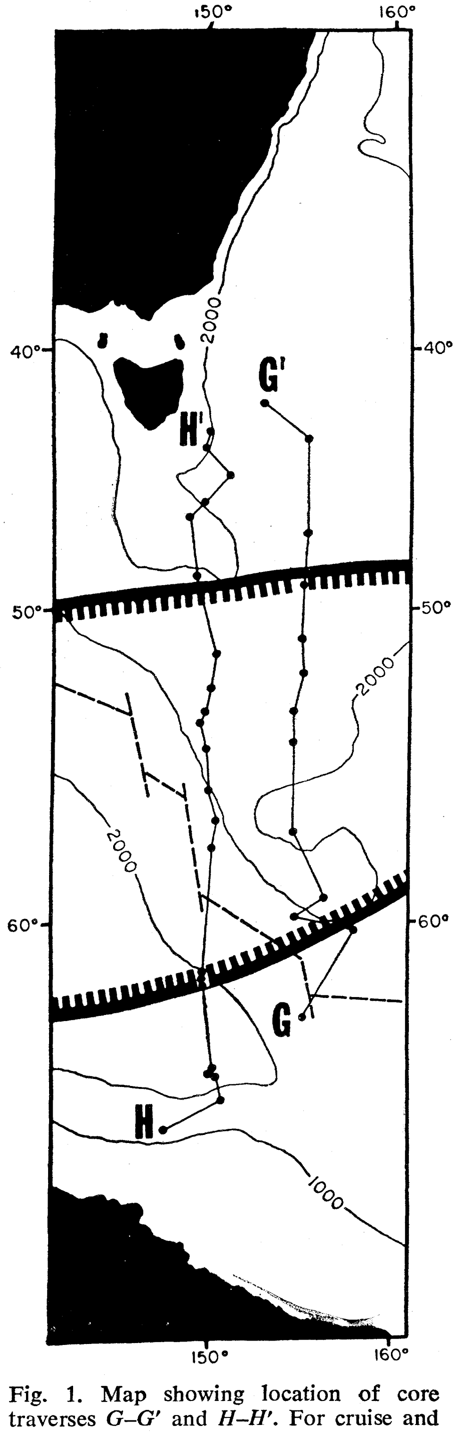

Fig. 1. Map showing location of core traverses *G–G'* and *H–H'*. For cruise and core numbers, see data in Fig. 2 and Table 1. Latitude is in degrees south; longitude is in degrees east. The 1000- and 2000-fathom bathymetric contours are shown. Fine dashed lines indicate the approximate positions of the ridge axis. Bold, hachured lines show the limits of the central zone of definite sediment removal by bottom currents.

It is clear from Fig. 1 that disconformities defined both paleomagnetically and micropaleontologically have been detected in many cores. Moreover, about 35 percent of the cores from the two traverses contain no Recent or Brunhes sediment, whereas at least four cores contain two disconformities. Furthermore, the major break in sedimentation in the Brunhes and Matuyama (Fig. 2) is not a random or local effect but is centered in the southern part of the Tasman Basin and northern flank of the Indian-Pacific Rise (Fig. 1). Uninterrupted sedimentary sequences are present to the north of the traverses on the south Tasman Ridge and within the central Tasman Basin, and to the south of the traverses nearer Antarctica. Hiatuses in sedimentation have previously been detected paleomagnetically in isolated cores (*11*) but have not been previously defined regionally in deep-sea areas.

Disconformities in deep-sea regions can result from three main processes: slumping, lack of sediment deposition, or submarine erosion. The disconformity is far too extensive (*12*) to have resulted from slumping and, furthermore, is centered in a basinal area rather than being confined to ridges. The formation of the disconformity entirely through lack of sedimentation is also untenable, because the area is in latitudes characterized by high biogenic productivity throughout the late Cenozoic.

There is strong evidence to indicate that deep-sea erosion has produced the disconformity. For instance, the upper few centimeters of numerous cores lacking Recent-Brunhes sediments are coarse residual sands or coarse accretionary sands (*4*) commonly made up of a mixture of micromanganese nodules, ice-rafted debris, fish teeth, robust Radiolaria and Foraminifera, and clay aggregates. Several cores in these surface sands contain reworked Radiolaria older than the underlying horizons. Clearly, these surface sands have been formed either by winnowing or reworking of coarse debris, or by both. According to the data of Gordon (*13*), topographic control has made the south Tasman Basin a major junction area of bottom currents from the South Australian Basin, the northern and central Tasman Basin, and the South Indian Basin (Fig. 3). It is not surprising, therefore, that high-velocity bottom currents (greater than 15 cm sec^{-1}) have been noted by Gordon in this general area. Such velocities are sufficient to remove material finer than fine sand size (< 0.2 mm) (*4*), and possibly even coarser sand-sized sedimentary fractions (*14*). The only important flow of bottom

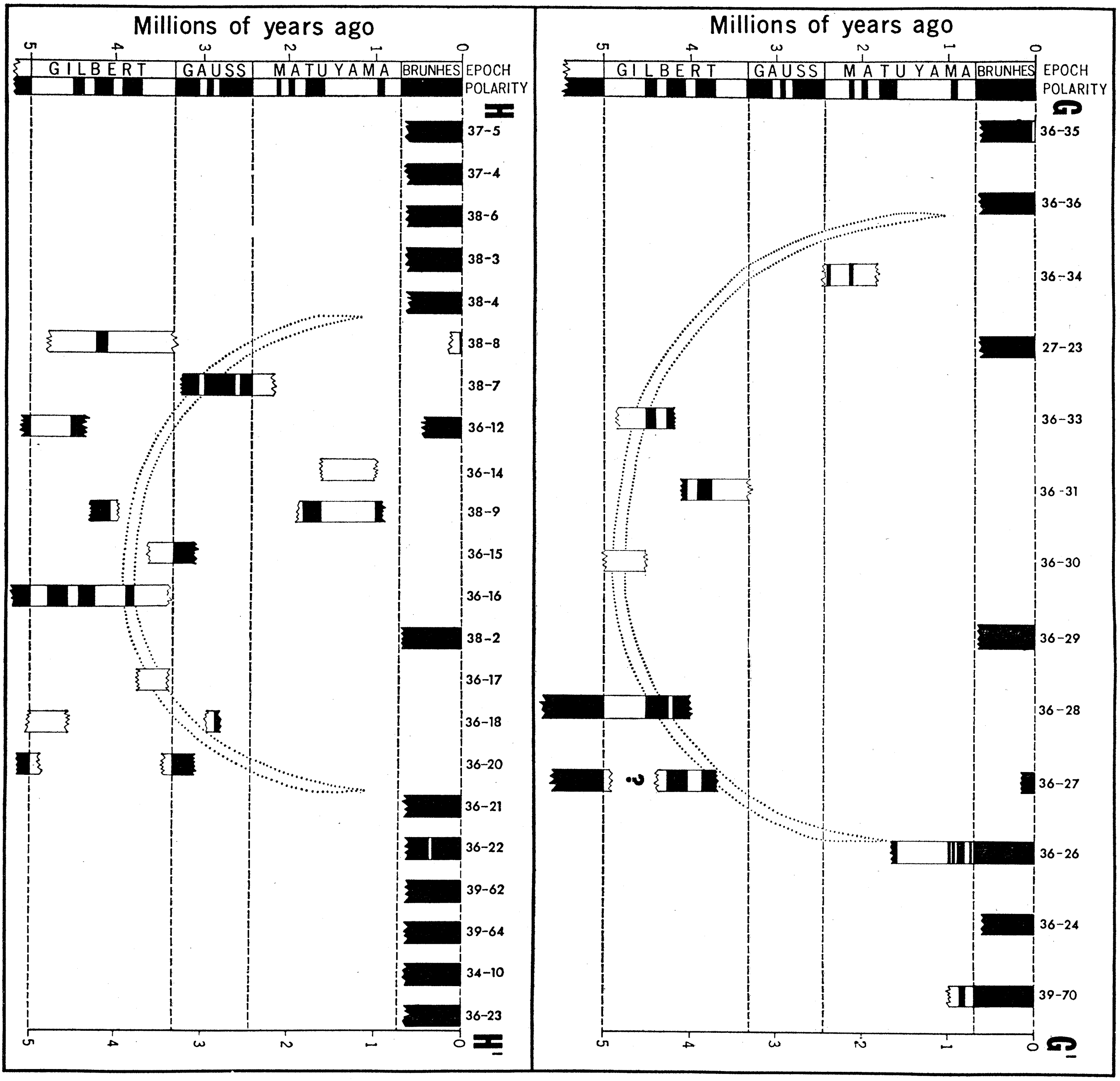

Fig. 2. Logs showing paleomagnetic data and time ranges of each core in the traverses shown in Fig. 1. At left are the known polarity history and polarity epochs (*7, 9*) (black, normal polarity; clear, reversed polarity). At the head of each log are the cruise and core numbers. Time ranges were determined by combining paleomagnetic and micropaleontological data [for limitations, see text and (*23*)]. The fine-dotted concave bowls represent the approximate ages of surface sediments based on cores from the two traverses (*5*).

water from the South Indian Basin to the Tasman Basin is across the Australian-Antarctic Rise immediately south of the Tasman Basin.

Sea-bottom features observable in bottom photographs (*15*) also provide substantial evidence of current activity in the region (Fig. 3). Sea-bottom photographs from the south Tasman Basin consistently show common to abundant manganese nodules and conspicuous ripple marks. In the central basinal region some scouring is evident. The photographs yield conspicuous evidence for bottom currents east and south of Macquarie Ridge (Fig. 3), where high-velocity currents have been measured directly (*16*). Other areas between Australia and Antarctica show evidence of much lower velocity bottom currents (Fig. 3). If 5 m of sediment is taken to represent the average amount of sediment removed over the area of the disconformity (approximately 3×10^6 km^2), then 1.5×10^{19} cm^3 of sediment has been removed. We speculate that the bulk of this vast volume of sediment has been transported by eastward-flowing bottom currents into the Emerald Basin of the southwest Pacific (Fig. 3). This speculation is clearly testable. Evidence of the scouring effect of the circumpolar current exists in the Bellingshausen Basin far to the east: Goodell and Watkins (*17*) have defined a west-to-east zone of low deposition rates by paleomagnetic means.

Despite the widespread nature of the sedimentary hiatus so defined, no sediments older than approximately 6 million years were found, and widespread sediments of Pliocene age, which accumulated at reasonable rates, are evident (Fig. 2). It is important to note that despite its vast areal extent, the disconformity represents the removal of only a few meters of sediment, most of which is of Brunhes and Matuyama epoch ($t = 0$ to 2.43 million years). We propose that only one explanation is possible for this situation: at some time in the latest Cenozoic, Antarctic bottom water has increased substantially in velocity. Studies of current velocities for erosion, transportation, and deposition (*4*) show that only particles larger than approximately 0.2 mm would remain deposited if current velocities are even only spasmodically greater than 20 cm sec^{-1}. A current system almost invariably less than 10 cm sec^{-1} is required for relatively continuous deposition of fine sediments. We therefore believe that there was an increase in bottom current velocities in this area from dominantly less than 10 cm sec^{-1} to dominantly more than 10 cm sec^{-1} during the latest Cenozoic, although it is highly probable that velocities have been spasmodically much greater during the period, to account for transportation of the coarsest sediments from the area.

A major factor contributing to preservation of sediment of Matuyama and older age but loss of much sediment of Brunhes age is, in our opinion, the change of cohesiveness of sediment with depth of burial. The older, more cohesive material would resist erosion by higher current velocities, which would nevertheless be effective in removing the younger, less cohesive material; a model of rapid sediment removal followed by marked slowing of the process is envisaged. Another factor contributing to the preservation of the older material is the creation of a manganese nodule pavement in the areas of nondeposition, which in turn would eventually inhibit erosion substantially. This factor is effective only in part of the area involved (Fig. 3) and must, therefore, be secondary. Core penetration is substantially less in the older sediment areas than in areas of Brunhes sedimentation (Fig. 1 and Table 1), and thus our concept of a critical increase in cohesiveness (and therefore resistance to erosion with depth) is supported. It appears that this critical increase must occur within 8 m of the surface in the cores under examination.

Table 1. Number, location, length, and water depth of cores used in this study.

Cruise No.	Core No.	Latitude (S)	Longitude (E)	Water depth (m)	Core length (m)
		Traverse G–G′			
36	35	62°44′	154°58′	3493	584
36	36	60°23′	157°32′	2817	572
36	34	59°59′	155°02′	2795	452
27	23	59°37.1′	155°14.3′	3182	955
36	33	57°45′	154°53′	3433	503
36	31	55°00′	155°00′	4271	461
36	30	54°04′	155°00′	4088	551
36	29	53°00′	155°10′	3905	500
36	28	51°35′	155°09′	4426	584
36	27	49°40′	155°	4536	1153
36	26	47°51′	155°08′	4691	1224
36	24	44°00′	155°00′	4549	569
39	70	42°23.8′	153°10′	4664	1673
		Traverse H–H′			
37	5	65°31′	147°26.3′	2990	684
37	4	64°49′	150°30′	3274	584
38	4	64°13.9′	150° 3.8′	3658	731
38	3	64°14.5′	150°01.3′	3493	943
38	6	64°17.5′	150°11′	3457	559
38	8	61°48.6′	149°54.2′	3292	544
38	7	61°49.3′	149°53′	3658	599
36	12	61°45′	149°33′	4057	603
36	14	58°06′	150°10′	3054	601
38	9	57°27.7′	150°06.3′	3173	610
36	15	56°34′	150°15′	3517	207
36	16	55°07′	150°00′	3823	590
38	2	54°14.1′	149°57.7′	4060	423
36	17	54°02′	150°05′	3951	612
36	18	53°00′	150°00′	3877	582
36	20	51°47′	150°27′	3863	541
36	21	49°27′	149°08′	3846	493
36	22	47°32′	148°01′	1103	422
39	62	46°56.8′	149°32.6′	3219	284
39	64	45°33.6′	150°21′	4653	453
34	10	44°31.6′	149°31.6′	2853	1186
36	23	43°53′	150°02′	2533	542

At this time insufficient evidence is available to determine with accuracy the time of initiation of the high bottom-current velocities that created the Recent disconformity. Variation in age of cores and disconformities throughout the region indicates that the history of bottom-current activity is not simple and is difficult to determine in detail because the minimum ages of most cores are a function of the degree of sediment erosion rather than a reflection of the initiation of current activities. Presence of disconformities with associated winnowed sediment horizons within the Gilbert epoch indicates that increased current activity did not commence suddenly but was active at times during the Gilbert, and that these periods of erosion were separated by periods of apparently normal biogenic sedimentation.

Based on the number of cores in the traverses containing normal biogenic and fine-grained sediments of Gilbert age (Fig. 2), the major late Cenozoic change in Antarctic bottom water probably took place during the post-Gilbert (since $t = 3.32$ million years) and possibly post-Gauss time (since $t = 2.43$ million years). Normal fine-grained biogenic sedimentation occurred during the Matuyama epoch on parts of the Australian-Antarctic Rise (cores E36-14, E38-9, and E36-34 in Fig. 2). This area, being more remote from the basinal areas, has been less affected by the bottom-current activities. Pockets of reworked Brunhes sediments occur within the basin but in some cases (for example, core E38-2, Fig. 2) consist of clays and robust reworked Radiolaria and Foraminifera of Brunhes age. Such cores indicate that high-velocity bottom currents have occurred during the Brunhes and that sediments containing Brunhes biogenic components have accumulated in isolated pockets. It appears, therefore, that Antarctic bottom water currents were active at times during the Gilbert epoch, became highly active at some time during post-Gilbert times, and have lasted until the Recent. Sedimentological analyses will undoubtedly refine this suggested history.

The major question posed by the inferred increase in velocities of Antarctic bottom water in the late Cenozoic is the cause of the change. Despite the obvious relation between topography and current systems, insufficient time has elapsed since deposition for changes in currents to result from substantial changes in submarine topography. Instead we propose that this increase in average current velocity is associated with a large change in the production of Antarctic bottom water from Antarctic ice. There is strong evidence for extensive glaciation of Antarctica in the late Cenozoic since at least the beginning of the Gilbert epoch ($t = 0$ to 5.0 million years) and for worldwide pre-Pleistocene cool climatic cycles assumed to be associated with increased glaciation of Antarctica (*18*). Periods of nonglaciation or partial glaciation of Antarctica result in decreased circulation of Antarctic waters, including decrease in magnitude of bottom circulation (*3*). It is, therefore, possible that ice development on the Antarctic continent reached a critical level during post-Gilbert or Gauss time. It is conceivable, for instance, that extensive, floating ice shelves developed at this time, and such shelves are likely to be important producers of Antarctic bottom water (*3*). It also follows that deep circulation may have experienced periods of even more highly intensified flow in response to more extreme climatic conditions associated with glacial periods and that deep circulation is now relatively quiescent (*19*). We suspect that the number of factors involved in our postulated change in current velocity is likely to be large: changes in latitudinal temperature gradients (*20*) and corresponding wind systems (*21*) would be substantial contributors to difference in current velocity with time.

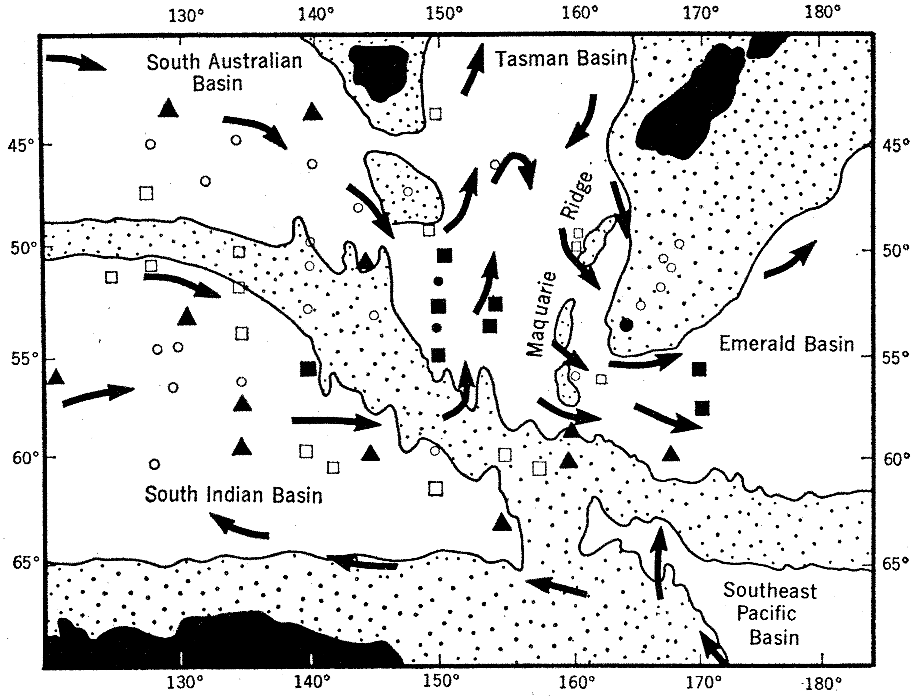

Fig. 3. Map of Southern Ocean between Australia–New Zealand and Antarctica showing circulation patterns of bottom waters and bottom-photograph (*15*) characteristics. Arrows represent bottom-water directions [from Gordon (*13*)]. Submarine ridge system is stippled. Symbols represent bottom-photograph characteristics as follows: □, abundant bioturbation; ○, bioturbation uncommon or absent; ▲, manganese nodules common; ■, manganese nodules abundant; ●, ripples and scour marks.

We consider that, in addition to the observed late Cenozoic disconformities, other disconformities certainly must exist in older parts of the sedimentary basins between Australia and Antarctica. The sediments of that part of the Southern Ocean between Antarctica and Australia are highly susceptible to changes in bottom-current velocity because of the general circulation and bottom topography. Australia and Antarctica separated perhaps as recently as 45 to 50 million years ago (*22*). Therefore, for much of the lower and middle Cenozoic, circumpolar currents including bottom waters were restricted to a relatively narrow channel and, hence, must have had very high current velocities. As Antarctica was glaciated during this same interval (*17*), circulation was probably vigorous, and the prospects of high current velocities in the area were therefore even more enhanced. Sediments recovered in any future deep-sea drilling operations will, in our opinion, include much coarse material, including concentrations of manganese nodules, in addition to numerous and widespread disconformities.

N. D. WATKINS
J. P. KENNETT
Graduate School of Oceanography,
University of Rhode Island, Kingston

References and Notes

1. For example, J. C. Ingle, Jr., *Bull. Amer. Paleontol.* **52**, 236 (1967); J. P. Kennett, *Deep-Sea Res.* **17**, 125 (1970); O. L. Bandy, R. E. Casey, R. C. Wright, in *Antarctic Oceanology I*, J. L. Reid, Ed. (American Geophysical Union, Washington, D.C., 1971), p. 1; D. B. Ericson and G. Wollin, *Science* **162**, 1227 (1968).
2. These changes have recently been summarized by E. J. W. Jones, M. Ewing, J. I. Ewing, and S. L. Eittreim [*J. Geophys. Res.* **75**, 1655 (1970)].
3. A. L. Gordon, in *Antarctic Oceanology I*, J. L. Reid, Ed. (American Geophysical Union, Washington, D.C., 1971), p. 169.
4. B. C. Heezen and C. D. Hollister, *Marine Geol.* **1**, 141 (1964).
5. N. D. Watkins and J. P. Kennett, "Paleomagnetic and micropaleontological definition of a sedimentary disconformity of regional extent in the Southwest Pacific," in *Antarctic Research Series*, D. E. Hayes, Ed. (American Geophysical Union, Washington, D.C., in preparation).
6. N. D. Watkins and H. G. Goodell, *Earth Planet. Sci. Lett.* **2**, 123 (1967); N. D. Watkins, *ibid.* **4**, 341 (1968).
7. A. Cox, *Science* **163**, 237 (1969).
8. N. D. Opdyke, B. Glass, J. D. Hays, J. Foster, *ibid.* **154**, 349 (1966).
9. J. D. Hays and N. D. Opdyke, *ibid.* **158**, 1001 (1967).
10. J. P. Kennett, *Deep-Sea Res.* **17**, 125 (1970).
11. For example: core A185 [B. Glass, D. B. Ericson, B. C. Heezen, N. D. Opdyke, J. A. Glass, *Nature* **216**, 437 (1967)]; core E32-51 [J. P. Kennett and N. D. Watkins, *ibid.* **227**, 930 (1970)]; core E13-4 [K. Geitzenauer, S. V. Margolis, D. Edwards, *Earth Planet. Sci. Lett.* **4**, 173 (1968)]; core CH61(171) [J. D. Phillips, W. A. Berggren, A. Bertels, D. Wall, *ibid.*, p. 118]. Many other examples can be found in the literature.
12. The disconformity is defined by traverse *A′–A* to *M′–M* (*5*). These range from latitude 120°E to 160°W.
13. A. L. Gordon, "Spreading of Antarctic bottom waters, II," in *Studies in Physical Oceanography—A Tribute to Georg Wüst on His Eightieth Birthday*, A. L. Gordon, Ed. (Gordon & Breach, New York, in press).
14. J. B. Southard, R. A. Young, C. D. Hollister, "Experimental erosion of calcareous ooze," *J. Geophys. Res.*, in press.
15. S. S. Jacobs, P. M. Bruchhausen, E. B. Bauer, Eds., *Eltanin Reports—Hydrographic Status, Bottom Photographs, Current Measurements: Cruises 32–36, 1968* (Lamont-Doherty Geological Observatory, Palisades, N.Y., 1970) for the U.S. Antarctic Research Program (National Science Foundation).
16. S. Eittreim, A. L. Gordon, M. Ewing, E. M. Thorndike, P. Bruchhausen, "The nepheloid layer and observed bottom currents in the Indian-Pacific-Antarctic Sea." in *Studies in Physical Oceanography—A Tribute to Georg Wüst on His Eightieth Birthday*, A. L. Gordon, Ed. (Gordon & Breach, New York, in press).
17. H. G. Goodell and N. D. Watkins, *Deep-Sea Res.* **15**, 89 (1968).
18. J. P. Kennett, *N.Z. J. Geol. Geophys.* **10**, 1051 (1967); S. V. Margolis and J. P. Kennett, *Amer. J. Sci.*, in press; O. L. Bandy, in *Tertiary Correlations and Climatic Changes in the Pacific*, K. Hatai, Ed. (Sasake, Sendai, Japan, 1967), p. 9; J. C. Ingle, Jr., *Bull. Amer. Paleontol.* **52**, 236 (1967).
19. D. A. Johnson, *Trans. Amer. Geophys. Union* **52**, 244 (1971).
20. C. H. Hendy and A. T. Wilson, *ibid.*, p. 229.
21. W. H. Munk, *J. Meteorol.* **7**, 79 (1950).
22. R. S. Dietz and J. C. Holden, *J. Geophys. Res.* **75**, 4939 (1970); *Sci. Amer.* **223** (4), 30 (1970); X. Le Pichon and J. R. Heirtzler, *J. Geophys. Res.* **73**, 2101 (1968).
23. In assigning time ranges for each core, nonlinear sedimentation rates (with which a perfect match of polarity scale and paleomagnetic data can obviously be forced) have not been assumed. This means that in the Gilbert epoch sediments in particular, a linear sediment rate based on two time-reference points has often resulted in imperfect matching of the polarity data and polarity scale. Therefore, although we believe that the time ranges are correct to ±0.4 million years, we are not certain of the correlation of many observed polarity events to the polarity scale, or the durations of the observed events.

24. Supported by NSF grants GA25400 and GV28305 (Office of Polar Programs).

30 April 1971; revised 28 June 1971 ■

Time, Energy, and Territoriality of the Anna Hummingbird (Calypte anna)

Abstract. *The male Anna Hummingbird accommodates seasonal changes in energy demands by varying its allocation of time and energy among different activities; total energy expenditures change relatively little. Augmented territorial defense during the breeding season is made possible by increased feeding efficiency due to the availability at this time of very nectar-rich flowers.*

A study of the way an organism budgets its available time and energy can provide valuable data for an ecological analysis of its behavior. Hummingbirds, because of their small size, are faced with relatively great problems of heat loss and energy balance. Time and energy studies of hummingbirds are therefore of particular ecological interest. Hummingbirds are also ideal subjects for the translation of time budgets into energy budgets since their active day is spent at essentially two distinct metabolic levels, perching and flight. (Most hummingbirds are incapable of terrestrial locomotion.)

Pearson (*1*) was the first to use physiological data to quantify the metabolic costs of various activities of a wild bird, a nonbreeding male Anna Hummingbird (*Calypte anna*). My objective in this report is to extend this analysis to other times of year and other ecological contexts, in order to determine the effects of reproduction and territoriality on the time and energy budget of the male Anna Hummingbird.

The bird observed by Pearson was holding a feeding territory; defense of flowers by male Anna Hummingbirds is common during the nonbreeding season (*2*). The size of the feeding territory varies with the density and nectar production of the flowers, and the level of competition (*3*). Most feeding territories are only a few square meters in extent; the surrounding area is not defended, and intruders are seldom pursued far beyond the bounds of the territory (*2*). During the breeding season male *C. anna* hold breeding territories consisting of a central "core area" of about 0.1 ha, and a surrounding "buffer zone" of up to 4 to 6 ha (*2, 4*). In breeding territories the area itself is defended rather than a food source, although the distribution of flowers is apparently important in the choice of a territory site by male *C. anna*. Breeding males engage in advertising flights, display dives, and frequent long chases in defense of their territories (*4*). In energetic terms, breeding territories thus appear to be much more expensive to defend than feeding territories.

Field observations were made in the Santa Monica Mountains, Los Angeles County, California. Breeding males were studied in February and March 1967, January through April 1968, and March 1969; males on feeding territories were observed in October 1968 (*5*). The basic method was continuous observation of wild birds for periods of from several hours up to a full day. The time of day and the length and nature of all bouts of activity were recorded. Activities were classified as perching (*P*), feeding at flowers (*F*), insect-catching by gleaning or hawking (*ic*), territorial aggression (*A*), miscellaneous flying (*f*), and out of contact (*ooc*). This last category includes time that the bird was out of my sight, hearing, or both, and almost always involved long flights beyond the bounds of the territory. Data on ambient (T_A) and black-bulb (T_{BB}) temperatures (*6*) and weather conditions were taken every 15 minutes in the field.

To obtain an accurate and meaningful time budget, one must study a bird whose activities are highly localized and visible, and all of whose territory and the surrounding area can be efficiently scanned. The abundances of flowers present in the territories of individual male *C. anna* differ greatly, and hence there are differences in the amount of time the birds must spend feeding elsewhere, often at considerable distances (*2*). I was unable to evaluate feeding activity for most males that fed to any considerable extent outside of their territories. Of necessity, I was restricted to intensive observation of those few individuals that met all these requirements. I obtained 69 hours of observations, including